ISSN (Print) 1226-1750
ISSN (Online) 2233-6656
Journal of Magnetics 22(2), 196-202 (2017) https://doi.org/10.4283/JMAG.2017.22.2.196

Finite Element Study of Ferroresonance in single-phase Transformers Considering Magnetic Hysteresis

Morteza Mikhak Beyranvand and Behrooz Rezaeealam*

Faculty of Engineering, Lorestan University, Lorestan, Iran

(Received 12 August 2016, Received in final form 3 May 2017, Accepted 4 May 2017)

The occurrence of ferroresonance in electrical systems including nonlinear inductors such as transformers will bring a lot of malicious damages. The intense ferromagnetic saturation of the iron core is the most influential factor in ferroresonance that makes nonsinusoidal current and voltage. So the nonlinear behavior modeling of the magnetic core is the most important challenge in the study of ferroresonance. In this paper, the ferroresonance phenomenon is investigated in a single phase transformer using the finite element method and considering the hysteresis loop. Jiles-Atherton (JA) inverse vector model is used for modeling the hysteresis loop, which provides the accurate nonlinear model of the transformer core. The steady-state analysis of ferroresonance is done while considering different capacitors in series with the no-load transformer. The accurate results from copper losses and iron losses are extracted as the most important specifications of transformers. The validity of the simulation results is confirmed by the corresponding experimental measurements.

Keywords : ferroresonance, finite element method, transformers, Jiles-Atherton (JA) vector model, power loss

1. Introduction

The ferroresonance is an oscillating phenomenon which occurs in an alternating electric circuit consisting of nonlinear inductor and capacitor. In the electrical systems, there are a large number of capacitors such as cables, long lines, capacitor-voltage transformers, series or shunt capacitor banks, voltage-grading capacitors in circuit breakers, metal clad substations, and the saturable inductors in the form of power transformers, voltage measurement inductive transformers (VT) and shunt reactors. The ferroresonance can cause the overvoltage and the overcurrent which highly distorts the waveforms of current and voltage and makes severe damages to equipment. Other ferroresonance effects are overheating in transformers and reactors, continuous and excessive loud sound and problems related to protection systems. All these phenomena and effects can be disastrous for the electrical systems [1, 2].

The ferroresonance is essentially a low-frequency phenomenon and generally has a frequency spectrum below 2 kHz. In general, the ferroresonance is classified as fundamental, subharmonic, and chaotic modes. The fundamental mode is characterized by the current and voltage waveforms with the frequency similar to the electrical system which can either have the harmonic content or not. In the subharmonic mode, current and voltage waveforms have submultiple frequencies of the power system frequency. The chaotic mode presents a wide spectrum of frequencies [2, 3]. The aim of the present work is accurate behavior investigation of transformer in the fundamental ferroresonance mode, which requires an accurate model of the transformer core.

Several research works based on the magnetic circuit analysis have been proposed for the ferroresonance analysis; for instance, a hysteresis model of an unloaded transformer has been introduced [1]. Analyzing the electromagnetic transients using the Preisach model of magnetic hysteresis has been done [4], and also a flux-current methodology using an inverse JA approach has been employed to model the hysteresis behavior of a nonlinear inductor [5]. However, magnetic circuit analysis does not allow considering the real dimensions of transformers and also the dynamic and nonlinear behavior of ferromagnetic core. Therefore, the accurate characteristics such as transformer losses can't be investigated. Although the ferroresonance phenomenon with the help of the Finite Element (FE) method for an autotransformer has been investigated

*Corresponding author: Tel: +98-66-33120005
Fax: +98-66-33120005, e-mail: rezaee.bh@lu.ac.ir

[6], but in this analysis the B-H curve is used to model the core which can't describe the actual nonlinear behavior of the core. Thus, in the present work an accurate nonlinear model of transformer core is proposed using the FE method and then the transformer characteristics will be investigated under the ferroresonance condition.

For the magnetic field analysis in electromagnetic devices, when the local magnetic field is rotating or if the materials have anisotropic property, the directions of magnetic flux density and magnetic field intensity are not parallel, but rather there is a lagging angle between B and H [7]. The interaction between B and H in such conditions can only be achieved using a vector model. Moreover, the losses due to the rotational flux has a significant share in the total loss of electromagnetic devices such as transformer. Thus, it is necessary to model the magnetic field in vector form [8, 9]. Preisach model and extensions of its original model have been used to effectively simulate the magnetic fields in recent years. However, taking account the rotation of the magnetic fields, the anisotropic vector Preisach model becomes more complex and the Preisach distribution function (PDF) has to be identified by measuring a set of reversal curves [10].

One of the famous methods for simulation of nonlinear characteristics of magnetic materials is the JA model. This model has been widely employed due to some advantages such as a relatively low number of physical parameters and little computational effort [11]. The JA hysteresis vector model using the magnetic differential reluctivity tensor is incorporated in the FE with vector potential formulation, which is more common than the numerical inversion model that the magnetic induction vector is used as the independent variable [12]. Thus, in the present work the JA inverse vector model is chosen.

2. JA Hysteresis Vector Model

In order to investigate the accurate behavior and characteristics of transformer in fundamental mode of ferroresonance, the FE method is used to analysis the transformer. The use of a vector model for modeling the nonlinear core allows the magnetic fields are applied in the principal directions so that the approximation of the average permeability in each FE is avoided, and the more realistic calculations are performed [8]. The JA inverse vector model chosen in this study is able to represent the anisotropic behavior of steel as well as the rotational flux in the T-joints of transformer. The transformer chosen in this work has the isotropic laminations and therefore the rotational flux in the transformer T-joints is considered by this method. This model reduces itself to a scalar model if the flux does not change its space direction.

2.1. Nonlinear model of core

Bergqvist proposed a generalized vector of the JA scalar hysteresis model that The JA vector model is able to represent isotropic and anisotropic electrical steels [12]. J. V. Leite and his colleague proposed reverse version of the original model equations [13]:

$$d\overline{M} = \frac{1}{\mu_0}[1 + f_\chi(1-\vec{\alpha}) + \vec{c}\vec{\xi}(1-\vec{\alpha})]^{-1} \cdot [f_\chi + \vec{c}\vec{\xi}]d\overline{B} \qquad (1)$$

with $f_\chi = \vec{\chi}_f |\vec{\chi}_f|^{-1} \vec{\chi}_f$ where the auxiliary variable $\vec{\chi}_f$ is defined by $\vec{\chi}_f = \vec{k}^{-1}(\overline{M}_{an} - \overline{M})$. $\overline{M}_{an}$ and $\overline{M}$ are respectively the anhysteretic magnetization and the total magnetization. I and $\vec{\xi}$ are the diagonal unity matrix and the diagonal matrix of the derivatives of anhysteretic functions, respectively. $\vec{k}$, $\vec{\alpha}$, and $\vec{c}$ are second rank tensors which must be obtained experimentally.

Using $d\overline{M}$ obtained from (1), can be written $d\overline{H} = \|\partial\nu\| d\overline{B}$, where $\|\partial\nu\|$ is the differential reluctivity tensor [8]. For the 3-D case the differential reluctivity tensor can be written as:

$$\|\partial\nu\| = \begin{bmatrix} \frac{dH_x}{dB_x} & \frac{dH_x}{dB_y} & \frac{dH_x}{dB_z} \\ \frac{dH_y}{dB_x} & \frac{dH_y}{dB_y} & \frac{dH_y}{dB_z} \\ \frac{dH_z}{dB_x} & \frac{dH_z}{dB_y} & \frac{dH_z}{dB_z} \end{bmatrix} = \begin{Vmatrix} \partial\nu_{xx} & \partial\nu_{xy} & \partial\nu_{xz} \\ \partial\nu_{yx} & \partial\nu_{yy} & \partial\nu_{yz} \\ \partial\nu_{zx} & \partial\nu_{zy} & \partial\nu_{zz} \end{Vmatrix} \qquad (2)$$

tensor terms in (2) are given in details in [13].

2.2. Voltage fed and magnetic vector potential formulation

By specifying the electric scalar potential V and magnetic vector potential $\overline{A}$, The formulation is obtained from the weak form of the Ampere's law [13]

$$\begin{aligned} &(\|\partial\nu\| \mathrm{rot}\overline{A}, (t, \Delta t)\mathrm{rot}\overline{A'})_\Omega - (\|\partial\nu\| \mathrm{rot}\overline{A}, \mathrm{rot}\overline{A'})_\Omega \\ &\quad + (\overline{H}(t), \mathrm{rot}\overline{A'})_\Omega + (\sigma\partial_t A, \overline{A'})_{\Omega c} + (\sigma \mathrm{grad} V, \overline{A'})_{\Omega c} \\ &\quad - (J, \overline{A'})_{\Omega s} = 0, \quad \forall \overline{A'} \in F_a(\Omega) \end{aligned} \qquad (3)$$

Where $F_a(\Omega)$ the function of space is defined on Ω which contains the basis functions for the vector potentials $\overline{A}$ and the test function $\overline{A'}$. The conducting regions of Ω is denoted as Ωc and the parts of stranded conductors is denoted as Ωs. The block $(.,.)_\Omega$ denotes the volume integral in Ω of produced scalar or vector fields. The electric field $\overline{E}$, the magnetic flux density $\overline{B}$, the magnetic field intensity $\overline{H}$, and the current density $\overline{J}$, are

denoted with terms of the magnetic vector potentials $\overline{A}$ and electric potential V by:

$$\overline{E} = \sigma^{-1}\overline{J} = -\partial t\overline{A} - \text{grad}V \text{ in } \Omega n \quad (4)$$

$$\overline{B} = \|\mu\|\overline{H} = \text{rot}\,\overline{A} \text{ in } \Omega \quad (5)$$

The circuit relation of the current I_j and voltage V_j associated with a stranded inductor $j \in \Omega s$ is denoted for the formulation of magnetic vector potentials $\overline{A}$:

$$\partial t(\overline{A}, \overline{w})_{\Omega s} + RI_j = -V_j \quad (6)$$

where R is the resistance of the inductor and $\overline{w}$ is the wire density vector that is defined as $\overline{w} = (N/S)\overline{U}$, where $\overline{U}$, N, S are respectively the unit vector in the coil direction, the turns number of the coil, and the inductor region.

In aforementioned equations, the magnetic vector potential $\overline{A}$ and coils currents are unknowns and the FE method is used to solve the problem.

3. Analyzed System

In this work, a single-phase transformer (shell-type custom-build isolating) is used. The main parameters and characteristics are: 1 kVA, 50 Hz, 400/400 V, the same windings in primary and secondary composed from 20 coils with 22 turns for each coil, the resistance and leakage inductance of primary, or secondary windings are respectively $R = 2.133\Omega$ and $L = 6.2$ mH. The geometrical specifications of the transformer are shown in Fig. 1.

Notably, GWINSTEK GDS-3254 digital oscilloscope is used to measure the current and voltage of transformer so that the hysteresis waveform is displayed with high precision. The schematic of test circuit and arrangement devices used in the lab, including transformer, different capacitors, measurement instruments and autotransformer can be seen in Fig. 2. To assure the security of the procedure in the lab against overvoltage and overcurrent and also direct measurement of voltage, the 66 turns of winding are chosen so that the transformer is fed with 60v. The notable point is that the range of capacitors required for the occurrence of the ferroresonance in this case is different from the ones required for the occurrence of the ferroresonance in the case that whole winding of transformer is fed with the rated voltage 400v, because the capacitor value required for the occurrence of the ferroresonance is a variable dependent on the voltage and current of the transformer.

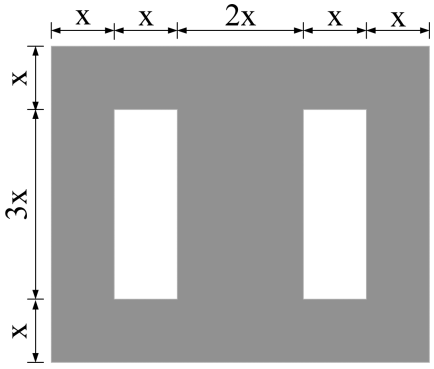

Fig. 1. Geometric size of the transformer core ($x = 28$ mm), (the core thickness = 100 mm).

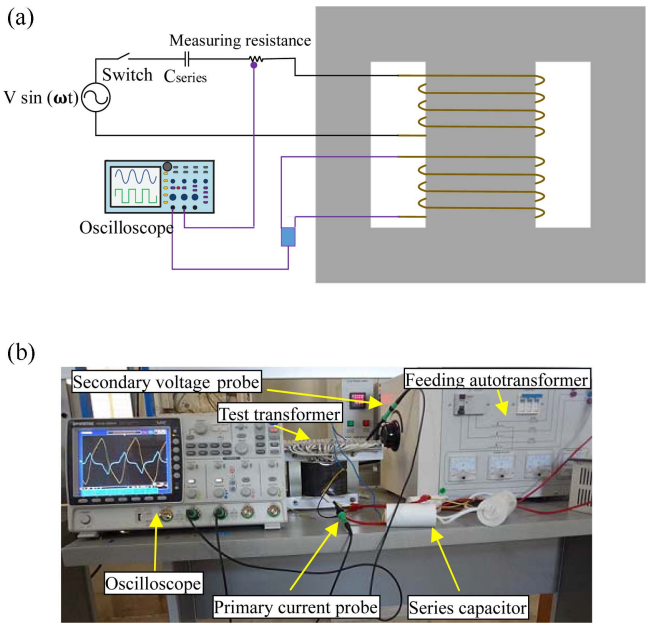

Fig. 2. (Color online) Experimental setup of the transformer (a) The circuit diagram; (b) The test bed setup.

4. Numerical Modeling of the Transformer

In this work, the JA inverse vector model is incorporated in 3-D FE for modeling the transformer. Because the ferroresonance occurs in an RLC circuit and its oscillation is highly dependent on all inductors and capacitors in the circuit, so a more realistic behavior of the coil leakage inductance is modeled by implementing 3D model, and the occurrence of the ferroresonance is modeled with more accuracy.

In this study, the JA reverse vector model is implemented via employing the COMSOL software package and using the magnetic differential reluctivity tensor incorporated with vector potential formulation. The capacitor is in series with the supply voltage applied to the primary winding of the transformer. The symmetrical structure of the transformer allows modeling one-eighth of the whole

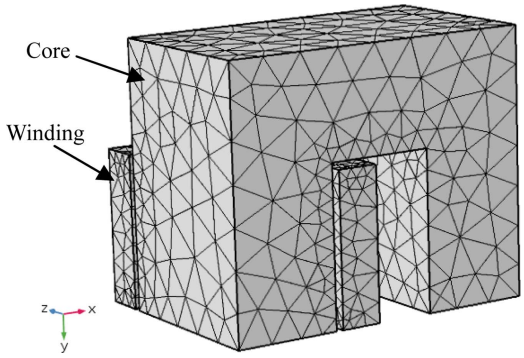

Fig. 3. (Color online) The three-dimensional model of the transformer.

region, as shown in Fig. 3, which leads to a reduction of simulation time.

One problem regarding the implementation of the JA model is to determine the corresponding coefficients for the electromagnetic device under investigation. Determining the coefficients of JA has been described in [14, 15]. Determining these coefficients for grain-oriented steel is more complex than the non-oriented one [16]. The analyzed transformer in this study is made of non-oriented Fe-Si electrical steel. The coefficients used for the transformer at no-load condition and without the capacitor are shown in Table 1.

Figure 4 shows the measured and calculated current waveforms under no-load condition with input voltage of 60v. It is clearly evident that the non-linear behavior of the transformer core leads to the non-sinusoidal current. The importance of considering the magnetic hysteresis in transformer modeling is illustrated in Figs. 4-5 that show the waveforms and harmonics components of current for

Table 1. The JA model parameters for the transformer core.

Parameter	M_s	K	c	a	α
value	1.64×10^{6}	523.4	441×10^{-3}	212.3	506×10^{-6}

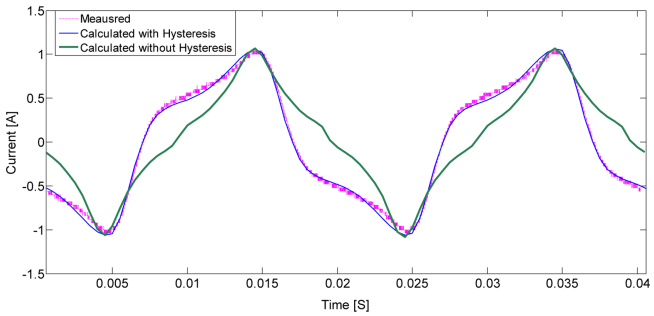

Fig. 4. (Color online) The measured and calculated current waveforms at no-load condition.

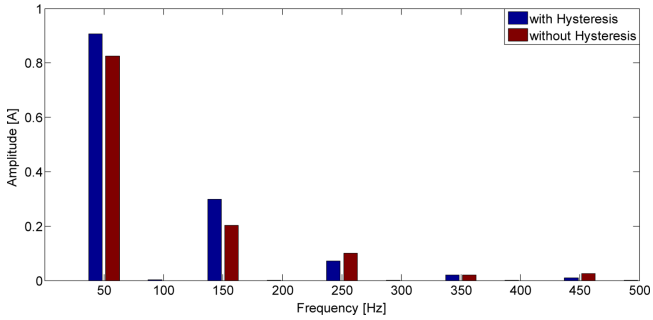

Fig. 5. (Color online) The harmonic content of current waveforms for the two cases of incorporating the magnetic hysteresis and the anhysteretic B-H curve.

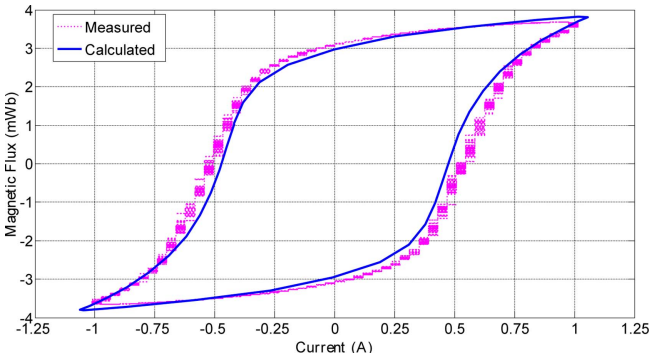

Fig. 6. (Color online) The calculated and measured hysteresis loop of the transformer.

the two cases of modeling using the magnetic hysteresis and also the anhysteretic B-H curve, it is seen that the current waveform obtained by employing the magnetic hysteresis model matches well with the measured current, in contrast to the one obtained using the anhysteretic B-H curve.

Now, to display the $\varphi - i$ hysteresis loop of the transformer under no-load condition, the current and the induced voltage in the windings are measured. For this purpose we measure the current of the primary winding, however, since the terminal voltage of the primary winding includes the leakage reactance voltage drop, so, it is easier to measure the open-circuit voltage of the secondary winding. It is noteworthy that the turn ratio between the primary and secondary windings is 1/1. Fig. 6 shows the calculated and measured hysteresis loop of the transformer. The JA coefficients are set in such a manner that the hysteresis loop derived by the 3-D simulation conforms to the measured one.

5. Simulation Results

In order to investigate the ferroresonance under the steady-state condition, the primary winding in series with

capacitor is fed with 60 V/50 Hz. Then, the capacitance is varied across the range 10 μF-300 μF in order to study the transformer specifications in the rated frequency, such as the voltage and current waveforms and their harmonic content, the core hysteresis loop, and the core losses. It is noteworthy that the JA coefficients should be adjusted for each capacitor value, so that the hysteresis loop implemented in the 3-D simulation matches with the measured hysteresis loop. Moreover, the residual magnetization is not included in the modeling.

In the absence of the capacitor, the copper loss and the core loss of the transformer are 0.14 W, 25.8 W, respectively. These losses severely change with the occurrence of ferroresonance. By changing the capacitance in series with the primary winding of the no-load transformer, the corresponding copper loss and core loss of the transformer are evaluated in the steady-state, and the results are shown in Figs. 7 and 8.

Figures 7 and 8 show that the capacitor of 220 μF causes the intense resonance and imposes the harshest conditions to the system, and lead to more losses in the transformer. In this work, the eddy current losses and the core additional losses are not considered, hence the core losses achieved through simulation is less than the measured core loss [17]. As the ferroresonance occurs, the core loss and copper loss increase dramatically, and it can be seen that the core losses are much larger than the copper loss. In the case of prolonged ferroresonance, thermal damages occur in the transformer and, therefore, it is necessary to use the grain-oriented steel instead of the non-oriented one, due to their much narrower hysteresis loop.

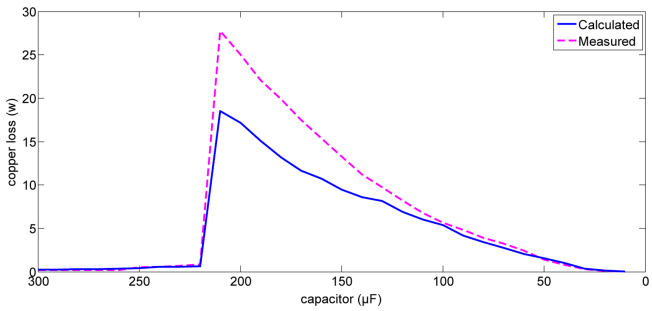

Fig. 7. (Color online) Copper losses versus the capacitance in series with the transformer.

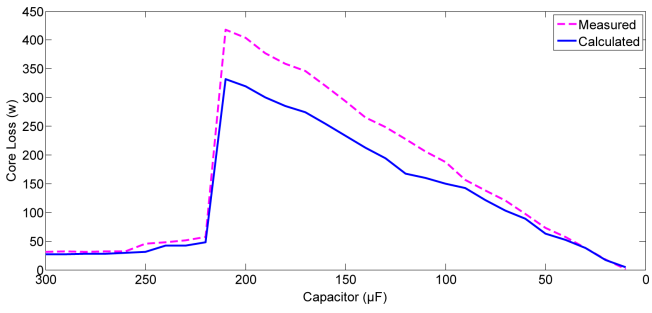

Fig. 8. (Color online) Core losses versus the capacitance in series with the transformer.

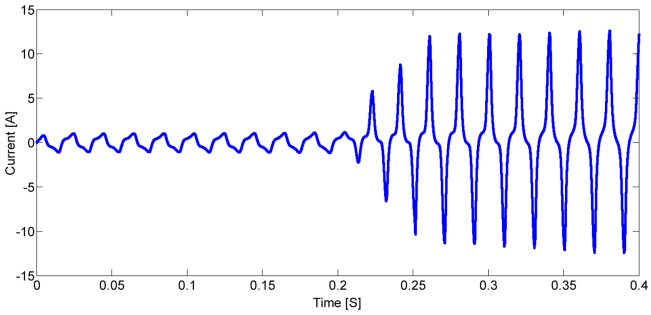

Fig. 9. (Color online) The current waveform of the Transformer (the series capacitor is inserted at $t = 0.2$ Sec).

For further inspection of the ferroresonance behavior of the transformer, the capacitor of 150 μF is connected in series with the unloaded transformer at time $t = 0.2$ Sec. Figure 9 shows that the current increases as ferroresonance occurs and the current waveform at steady-state and its harmonic content, magnetic hysteresis loop and flux density distribution are shown in Figs. 10 to 12, respec-

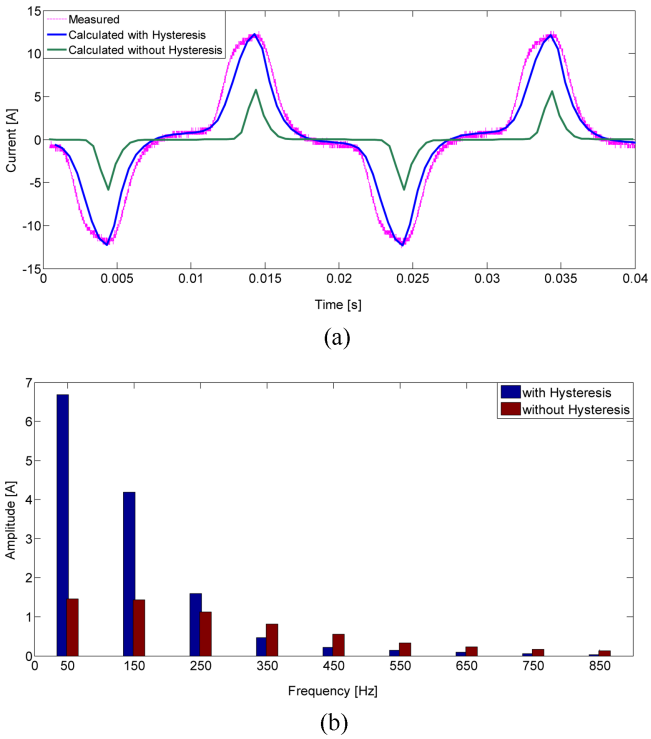

Fig. 10. (Color online) The measured and calculated current waveforms of the unloaded transformer for $C = 150$ μF. (a) The current waveform. (b) The FFT of the waveforms.

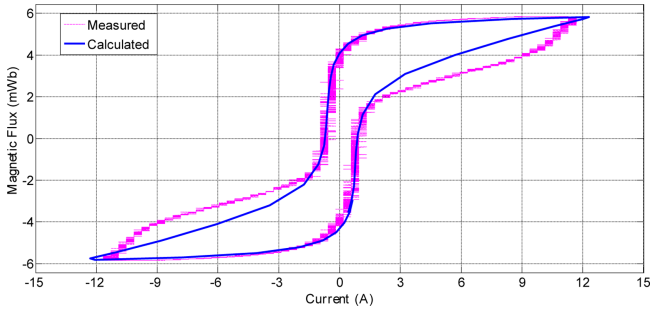

Fig. 11. (Color online) The measured and calculated hysteresis loop of the unloaded transformer for $C = 150\ \mu F$.

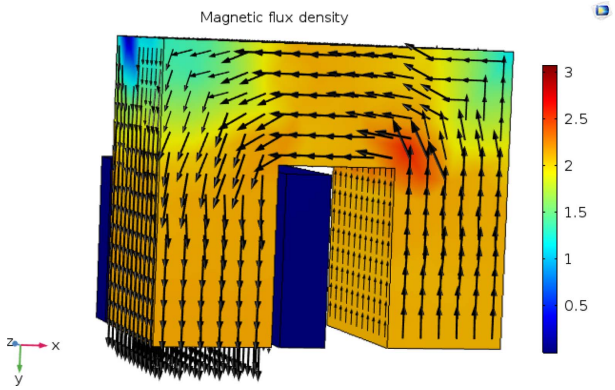

Fig. 12. (Color online) The magnetic flux density of the unloaded transformer for $C = 150\ \mu F$.

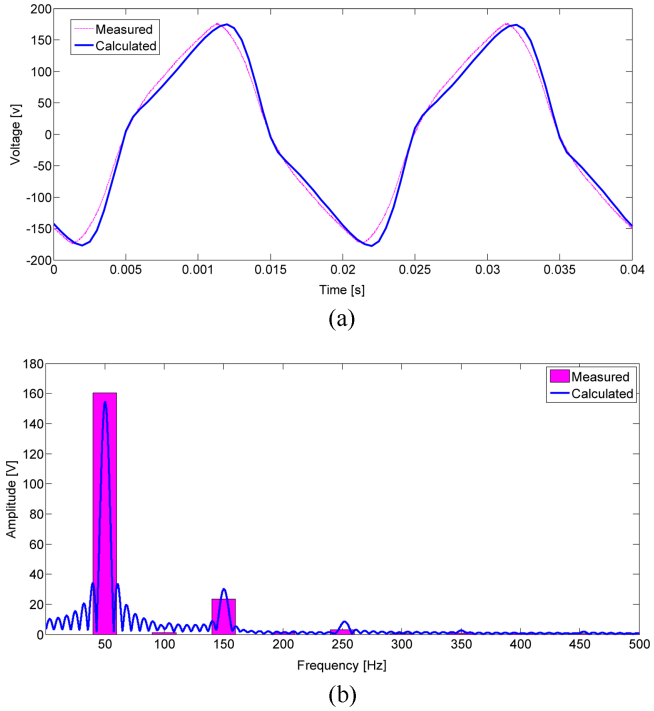

Fig. 13. (Color online) The measured and calculated output voltage of the unloaded transformer $C = 150\ \mu F$. (a) The voltage waveform; (b) The FFT of the voltage waveform.

tively. The sharp rise in current, higher-order harmonics (especially the third and fifth harmonic), the enlargement of the hysteresis loop and the severe saturation of the core are clearly observed in these figures.

Also, the voltage waveform is distorted when ferroresonance occurs, as shown in Fig. 13. Thus, it is essential to analyze the harmonic content of the output voltage of the transformer. Figure 13b shows that the fundamental, third and fifth harmonics are the dominant harmonics when ferroresonance occurs, and also in comparison with the input supply voltage of 60 V, the fundamental harmonic of the output voltage severely increases under the steady-state condition of the prolonged ferroresonance.

6. Conclusion

The no-load transformer was accurately modeled by using 3D finite element method, taking into account the JA hysteresis reverse vector model, as the simulation results were in good agreement with measurements. Ferroresonance causes a huge increase in the power losses of the transformer, mainly in the core losses that is due to the widened magnetic hysteresis loop and severe saturation. This highlights the importance of employing grain-oriented electrical steels in power transformers, because of their much narrower hysteresis loop. Moreover, the output voltage of the transformer becomes non-sinusoidal and much higher than the input supply voltage.

References

[1] B. Patel, S. Das, C. K. Roy, and M. Roy, TENCON 2008-2008 IEEE Region 10 Conference, IEEE (2008) pp. 1-6.
[2] H. Lamba, M. Grinfeld, S. McKee, and R. Simpson, IEEE Trans. Magn. **5**, 2495 (1997).
[3] P. Ferracci, Ferroresonance, Cahier Technique n. 190 :2, Groupe Schneider (1998).
[4] A. Rezaei-Zare, R. Iravani, M. Sanaye-Pasand, H. Mohseni, and S. Farhangi, IEEE Trans. Power Delivery **3**, 1448 (2008).
[5] J. C. Lacerda Ribas, E. M. Lourenco, J. Vianei Leite, and N. Batistela, IEEE Trans. Magn. **5**, 1797 (2013).
[6] C. A. Charalambos, Z. D. Wang, P. Jarman, and M. Osborne, IEEE Trans. Power Delivery **3**, 1275 (2009).
[7] X. Wang, D. Xie, B. Bai, N. Takahashi, and S. Yang, IEEE Trans. Magn. **6**, 890 (2008).
[8] J. V. Leite, A. Benabou, N. Sadowski, and M. V. F. Da Luz, IEEE Trans. Magn. **3**, 1716 (2009).
[9] T. D. Kefalas, G. Loizos, and A. G. Kladas, IEEE Trans. Magn. **5**, 1058 (2011).
[10] I. D. Mayergoyz and G. Friedman, IEEE Trans. Magn. **6**, 2928 (1988).

[11] D. C. Jiles and D. L. Atherton, J. Magn. Magn. Mater. **1**, 48 (1986).
[12] A. J. Bergqvist, IEEE Trans. Magn. **5**, 4213 (1996).
[13] J. V. Leite, N. Sadowski, P. Kuo-Peng, N. J. Batistela, and J. P. A. Bastos, IEEE Trans. Magn. **4**, 1769 (2004).
[14] J. P. A. Bastos and N. Sadowski, ISBN: 0-8247-4269-9, Marcel Dekker Inc., New York (2003).
[15] K. Chwastek and J. Szczygłowski, 2nd Symposium on Applied Electromagnetics, Przegląd Elektrotechniczny, Poland (2008) pp. 33-40.
[16] L. S. Coelho, F. Guerra, N. J. Batistela, and J. V. Leite, IEEE Trans. Magn. **5**, 1745 (2013).
[17] M. V. F. D. Luz, J. V. Leite, A. Benabou, and N. Sadowski, IEEE Trans. Magn. **8**, 3201 (2010).